Fused Deposition of Ceramics (FDC) for Structural Silicon Nitride Components

M.K. Agarwala, A. Bandyopadhyay, R. van Weeren, N.A. Langrana*, A. Safari, and S.C. Danforth
Center for Ceramic Research and *Dept. of Mechanical Engineering
Rutgers - The State University, Piscataway, NJ.

V. R. Jamalabad, P. J. Whalen, R. Donaldson, and J. Pollinger
AlliedSignal Inc., Morristown, NJ.

Fused Deposition of Ceramics is an SFF technique based on commercial FDM™ technology, for fabrication of structural and functional ceramic components. This study describes, in detail, process improvements made in pre-FDC, FDC, and post-FDC fabrication steps to achieve functional properties in commercial GS-44 silicon nitride components. Microstructural characterization of sintered FDC parts reveals microstructures similar to conventionally processed silicon nitride material. Mechanical properties of FDC processed silicon nitride bend bars and toughness samples were evaluated. These property evaluation studies demonstrate that mechanical properties similar to commercial GS-44 silicon nitride materials can be achieved using FDC. The study also describes results achieved on fabrication of complex components from silicon nitride using FDC.

I. Introduction

Most of the SFF techniques have been commercialized for fabrication of polymer and plastic parts for design verification and form and fit. Recently, some of these techniques are being explored for fabrication of structural metal and ceramic components [1]. Direct fabrication of parts and molds from metals and ceramics using the SFF techniques has created an opportunity to reduce lead times and costs in the development of new products. Such an opportunity for manufacture of new ceramic parts in a matter of days offers several advantages over conventional ceramic processing which can take weeks or months to produce the parts or complex tooling for the parts. The ability to do cost effective, iterative design using SFF techniques enables designers to create components using ceramic design guidelines from the start rather than components designed for metals. Some of these SFF techniques have been developed for ceramic part manufacture and are commercially used in production of parts [1]. One such technique called Fused Deposition of Ceramics (FDC) has been developed and demonstrated for structural ceramics [2-6]. FDC is based on an existing Fused Deposition Modeling (FDM™) technology, commercialized by Stratasys Inc., for processing of polymers and waxes [1,7,8].

Fused Deposition of Ceramics (FDC)

Fused Deposition of Ceramics (FDC) has been developed to create functional ceramic components using ceramic-polymer feedstocks [2-4]. These feedstocks are extruded into filaments of 0.070" nominal diameter, which are then used as the feed material for fabrication of three-dimensional green ceramic objects using a commercial FDM™ system, 3D Modeler™. During FDC processing, the polymer/wax acts as a carrier and binder for the ceramic particles as the material flows out of the heated extruder head. The green ceramic object thus created is then subjected to conventional binder removal and sintering processes, to produce fully dense structural ceramic components. As in the case of any manufacturing process, there are several inter-related process variables which determine the success and quality of parts fabricated by FDM™ and FDC processes. Poor control and optimization of these variables results in the presence of flaws/voids in the parts which are detrimental to the structural properties of the part.

The FDM™ process was originally designed for wax and polymer materials to serve the purposes of form and fit and positives for investment casting. Consequently, of chief importance to the end users is the external dimensional accuracy and to some extent, surface finish of the final parts. The presence of internal defects in parts built by FDM™ has not been a priority in the development of the FDM™ process. The prevention or elimination of these defects, such that ceramic components with functional engineering properties could be made by FDC, is the focus of current FDC research [5,6]. As will be shown here, structural properties have been obtained in a commercial grade silicon nitride through process control at every stage of the FDC process. Further, it is shown that it is possible to rapidly fabricate complex shaped ceramic components.

II. Development of Green Filaments for FDC

Successful FDC processing starts with fabricating filaments of 0.070" ± 0.001" diameter to be used as feed material in the FD hardware. However, for a filament material to be suitable for FD processing, it must possess certain thermal and mechanical properties [4,8]. The key variables that require careful attention and simultaneous optimization in developing the filaments for FDC processing are: viscosity and adhesion behavior of the material, and the flexural modulus and strength of the filaments. By tailoring the ceramic particle characteristics and/or binder chemistry the properties can be optimized in ways similar to that used by the ceramic injection molding industry. Based on the constraints imposed by these variables for FDC processing, a series of thermoplastic binders have been developed to enable FDC processing. These binders, called the RU series of binders, are four component systems in which the amount of each component was tailored to achieve appropriate viscosity, adhesion behavior, flexibility and stiffness in the final ceramic filament. Table I shows the four components of the RU series of binder, the role each component plays in the mixed system, and weight percent range of each component. Appropriate tailoring of these components along with the selection of a suitable surfactant for the specific particle system being used have enabled FDC processing of several ceramic systems [3].

The work reported here is based on FDC using an *in-situ* reinforced silicon nitride, referred to as GS-44[*]. The GS-44 powder is pre-treated with 3 weight % oleyl alcohol which serves as an appropriate dispersant for GS-44 [4]. RU9 and RU11 binder formulations were used in this study for GS-44. RU9 formulation contains 20.25% wax, 18.75% polymer, 34.5% tackifier, and 26.5% elastomer while the RU11 formulation contains 27% wax, 30% polymer, 21% tackifier, and 22% elastomer by weight. Mixing of the required amount of GS-44 powder, pre-treated with dispersant, with the binders was done using a torque rheometer mixer. GS-44/binder feedstocks containing 55 volume % GS-44 were used for FDC processing. The compounded feedstock was granulated and sieved for filament extrusion. Continuous lengths of 0.070" ± 0.001" diameter flexible filaments were fabricated using a single screw extruder and wound onto a spool [4].

III. FDC Processing

FDC processing, using commercial FDM™ systems, employs the same build strategies used in FDM™ processing of polymers. First, material is deposited as a perimeter defining the boundaries of a given layer of the part followed by raster motion of the liquefier head depositing material inside these boundaries as a series of adjacent roads. This two step strategy is repeated layer-by-layer, creating a three-dimensional green ceramic part. Therefore, any debonding between adjacent roads and adjacent layers, or incomplete filling of any regions of the part will result in property limiting defects in the final sintered ceramic parts. Strength or property limiting defects in FD processed parts have three primary causes.

---

[*] AlliedSignal Ceramic Components, Torrance, California

- Surface defects such as, surface finish, stair step formation, etc. due to limitations in the current state of all SFF technologies.

- *Internal defects due to poor optimization of feed filament material, i.e. non-uniform flow rate.*

- Internal defects due to current FDM™ hardware and software limitations.

Surface defects arising in FDC parts due to poor surface finish inherent to SFF processing have been eliminated via post-FDC surface finishing operations, as is a common practice in most SFF processing applications. As shown in Figure 1, the green FDC GS-44 Si_3N_4 parts fabricated using RU binders do not exhibit any delamination or any debonding between adjacent roads. Microstructurally, individual roads and layers are indistinguishable in the green state. Several internal defects were, however, observed in the early FDC processed parts. Defects arising due to poor control of filament diameter and poor FDC process optimization have been eliminated by better control of filament diameter (to ± 0.001") during fabrication by single screw extrusion and by optimization of FDC processing conditions. However, two key defects remained, namely, sub-perimeter voids and inter-road defects. These were largely due to limitations in the current FDM™ build strategy and FDM™ system hardware and software. Defects arising due to these limitations have also been observed in commercial FDM™ wax and polymer materials [5].

Sub-Perimeter Voids: During raster filling of a layer, voids are left due to incomplete filling at points where the raster segment turns around at the perimeter. The FDM™ system generates tool paths with sharp turns in the build file for complete filling at these locations. However, due to the constant velocity of the liquefier, the actual liquefier tool path during deposition is curved. The result of such an action is incomplete material fill at these intersections. The size and occurrence of the sub-perimeter void depends on the build conditions (road width and thickness, and liquefier head speed) and the angle between the raster line and the perimeter curve [6]. Figure 2 shows schematically how these voids are created and strategies that have been implemented to eliminate them, discussed below.

Since sub-perimeter voids are predictable and the cause of their existence is known exactly, several solutions are feasible for eliminating them. A simple way of eliminating these defects is to give a negative offset to the perimeter. This results in the liquefier head "plowing" into the perimeter during raster motion, as shown in Figure 2b, ensuring void-free parts. However, the negative offset to the perimeter needs to be optimized for each build condition such that the "plowing" action does not result in excessive flow of material at these locations. An alternative solution is to alter the tool path such that the actual tool path does not leave any unfilled regions. This approach includes extending the corners of raster segment turns, at the perimeter, closer to the perimeter [6], Figure 2c. Such a change in the tool path in the build file results in an actual tool path motion which is a closer approximation of the sharp turn rather than the curved turn. This solution of altering the path of raster segment at the intersection with the perimeter has recently been developed and implemented successfully for FDC.

Inter-Road Defects: Defects between adjacent roads (inter-road defects) can occur in one of two following forms : 1) if there is no physical contact between adjacent roads, defects will be present as voids between adjacent roads, which can be easily observed in the green state, or 2) if there is physical contact between adjacent roads but the bonding between them is not strong, then the defect between adjacent roads may be present as a weak interface. Such a weak interface is not easily observed in the green state but can cause serious damage to the structural integrity of the part during binder removal and/or sintering. These inter-road defects result from various sources.

Poor bonding between adjacent roads can arise from inconsistent material flow due to variation in filament diameter or filament slippage between rollers. This has been overcome by fabrication of filaments with controlled diameter and by optimization of the roller drive system,

respectively. Inter-road defects also arise due to excessive cooling of previously deposited adjacent roads when the road vector length is large. This is analogous to poor sintering between adjacent scan lines in SLS or print lines in 3D Printing when the vector lengths are large [1]. As done in SLS and 3D Printing, bonding between long vector length raster segments in FDC parts has been improved by providing a negative gap between roads such that the roads partially overlap. Further improvements in inter-road bonding have been made by optimizing the build environment temperature and optimization of the amount of tackifier in the binder chemistry to provide for optimum adhesion and hence bonding characteristic.

Defect Free FDC Processing: A series of square cross-section (1/2" X 1/2") bars were fabricated using a slice thickness of 0.01", road width of 0.02", negative gap between roads of 0.002" and a negative offset was provided to the perimeters to account for the sub-perimeter voids. FDC of GS-44/RU binder systems was done at 150°C-155°C at a liquefier head speed of 0.5"/second. These bars were then used for mechanical property evaluations after binder removal and sintering. Fabrication of complex components by FDC was demonstrated by fabrication of a top section of a tactical missile radome. The radome .stl file was scaled up by 20% in all three directions to accommodate the shrinkage during sintering and surface finishing operations. The file was then sliced using a slice thickness of 0.01" and then truncated in the Z-direction to obtain only the top 4.8" of the scaled-up version of the radome. The scaled-up radome had a base diameter of 3.1", wall thickness of 0.075" and an angle of inclination of approximately 72°. The green radome was fabricated in 12 hours without the need for any support structure using the same FDC conditions used for 1/2" square bars mentioned above. However, no negative gap was provided between roads as the vector lengths of raster segments were short enough to allow complete inter-road bonding. In addition to bars and radome, several other simple and complex shaped parts were fabricated, Figure 3.

IV. Binder Removal and Sintering of FDC Parts

As mentioned earlier, the RU family of binders being used for FDC are multi-component with different thermal degradation temperature ranges, Table I. For these binder systems, binder removal was done in two stages. In the first stage (room temperature to 450°C), 90 to 95 weight % of the binder was removed in a flowing nitrogen environment. During this stage, different heating rates were used in different temperature intervals to prevent surface as well as internal cracking of the samples. At low temperatures (< 200 °C), liquid binder component(s) were removed via capillary action to the surrounding setter bed material of activated charcoal, in a process called wicking. Such a loss of binder by capillary action creates surface connected internal pore channels that make further removal of binder much easier and prevents sample cracking during the process. At a higher temperature (200°C to 450°C), the remaining binder was removed by evaporation and decomposition. The residual binder (5 to 10 weight %) after the first stage, mostly present in the form of carbon, was removed in the second stage of the binder removal process by placing the sample in an alumina crucible without any setter bed and heating in air to 500 °C. The heating rate and the soaking time at different stages are dependent on the size and shape of the part. The maximum cross-section FDC samples which have been successfully processed for binder removal without any defects are currently limited to 1/2"X1/2".

The GS-44 raw material powder contains primarily $\alpha-Si_3N_4$ and a small volume (<10%) of oxide sintering aids. During high temperature gas pressure sintering, these oxide additives melt and provide a liquid phase for densification of the porous compact. As densification proceeds, the $\alpha-Si_3N_4$ transforms to $\beta-Si_3N_4$ through a solution-reprecipitation process. When densification is complete, the sintering aids remain in the grain boundaries as amorphous phases. Sintering of the radome section was done in a machined graphite fixture to prevent any deformation of the part.

V. Physical and Mechanical Properties

Density: The properties of green, brown, and sintered FDC square cross-section bars were compared with similar bars fabricated by extrusion of GS-44 bars with the same binder chemistry used for FDC. Binder removal and sintering procedures for extruded bars were the same as those for FDC parts. Iso-pressed GS-44 samples were used as control samples for property comparison with FDC and extruded samples, since iso-pressing of GS-44 is a conventional manufacturing approach for GS-44 silicon nitride components. Bulk densities of green FDC parts initially were 85%-90% due to internal build defects arising from FDM™ build strategy, discussed earlier. After implementation of novel strategies to eliminate the FDM™ related build defects, the bulk densities of green FDC parts were consistently greater than 96%. As shown in Table II, the sintered densities of FDC samples, after implementation of strategies to eliminate build defects, were comparable to those of extruded and iso-pressed samples.

Shrinkage: Shrinkage measurements in FDC samples were made to detect anisotropy between the build plane (X-Y plane) and the build direction (Z axis). Significant anisotropic shrinkage behavior is commonly observed in parts fabricated by SFF techniques where the shrinkage is greater in the build direction than in the build plane [1]. In the FDC samples in this study, a similar anisotropic shrinkage behavior was observed between the build direction and the build plane. Before elimination of FDM™ related build defects, the linear sintering shrinkage in the build plane was 12-15% while that in the build direction was 17-20%. However, after implementation of the defect eliminating strategies, this anisotropy in shrinkage has been reduced with average build plane shrinkage of $16.6 \pm 1.3\%$ and the build direction shrinkage of $19.3 \pm 1.6\%$. It has been observed that the degree of anisotropy in shrinkage is directly related to the total defect population in the parts. Parts with low defect population exhibit a smaller degree of anisotropy in shrinkage compared to parts with higher defect population, since most of the defects typically exist between layers. Therefore, as the defect population decreases, the parts' greater isotropy in the green state translates to more isotropic shrinkage upon sintering. Sintered samples with densities greater than 98% theoretical density show a difference of 2-3% in shrinkage between the build direction and build plane, which is far less than reported by other SFF techniques, suggesting a more uniform microstructure in FDC processed green parts.

Mechanical Property: ASTM MilSpec B 4-point bend tests were conducted on samples machined from extruded, FDC and iso-pressed GS-44 bars. As shown in Table II, average bend strengths of 824 ± 110 MPa measured for FDC samples are comparable to those for extruded and iso-pressed samples. Three point bend test were also carried out with indented samples where an indentation was created by applying a 20 Kg load using a Vickers indentor on the tensile surface of the sample. This test gives a qualitative idea of the fracture toughness of the samples where a higher failure strength indicates a higher fracture toughness. As shown in Table II, average indented failure strengths indicate similar fracture toughness behavior for FDC, extruded and iso-pressed samples.

Microstructure: Sintered FDC parts were observed under optical and scanning electron microscopes (SEM) to evaluate the microstructures for the following : (a) FDC build related defects, (b) delamination during binder removal and sintering, (c) evidence of road and layerwise build strategies, and (d) GS-44 Si_3N_4 microstructure. Figure 4 shows SEM fractographs of FDC and iso-pressed samples tested under indented three point bend loading. Although some FD defects can be observed on the fracture surfaces of FDC samples, they didn't have a significant effect on the failure strength. Other than a few FD related defects, the fracture surfaces of conventionally and FDC processed samples appear similar. The microstructures in the directions perpendicular and parallel to build direction were similar. Individual roads and layers were indistinguishable. There were no discernible signs of layerwise fabrication.

As shown in Figure 5, the sintered FDC radome section maintained its overall conical shape and straight sides with a sintered angle of inclination of 71°. The sintered wall thickness was 0.065" accounting for 13.3% linear shrinkage in X-Y build plane. The sintered base diameter was 2.6" leading to measured shrinkage in the diameter at base of 16.1%. The shrinkage in build direction (Z) of 20.8% was slightly greater than expected shrinkage of 20%, with the final vertical height of 3.8". Although, the density of the radome was measured to be greater than 98% of theoretical density of GS-44, several defects were observed on the surface and internally, detected using X-ray radiography. Most of these defects were primarily due to the FD build approach used.

VI. Conclusions

GS-44 silicon nitride parts have been formed using a new method, Fused Deposition of Ceramics, FDC. Simple and complex shapes have been produced with high green density after most of the FDC build defects were eliminated. The process has been developed to produce green parts with largely defect-free internal microstructures. It has been demonstrated that FDC green parts can have the binder removed and be sintered to densities and strengths comparable to those produced by conventional ceramic processing approaches. Development of such a process as FDC will enable ceramic design engineers to rapidly fabricate complex shapes and verify the design for not only form and fit but also for performance.

Acknowledgments

References

1. Proceedings of the Solid Freeform Fabrication Symposium, Vol. 1990, 1991, 1992, 1993, 1994, 1995, Edited by H.L. Marcus, J.J. Beaman, J.W. Barlow, D.L. Bourell, and R.H. Crawford, The University of Texas at Austin, Austin, Texas.
2. M.K. Agarwala, et. al., "Structural Ceramics by Fused Deposition of Ceramics," ibid., Reference #1, Vol. 6, 1995, pp.1-8.
3. M.K. Agarwala, et. al., "Fused Deposition of Ceramics and Metals: An Overview," ibid., Reference #1, Vol. 7, 1996.
4. M.K. Agarwala, et. al., "Filament Feed Material for Fused Deposition Processing of Ceramics and Metals," ibid., Reference #1, Vol. 7, 1996.
5. R. van Weeren, et. al., "Quality of Parts Processed by Fused Deposition," ibid., Reference #1, Vol. 6, 1995, pp. 314-321.
6. V. Jamalabad, M.K. Agarwala, N. Langrana, and S.C. Danforth, "Process Improvements in the Fused Deposition of Ceramics (FDC) : Progress Towards Structurally Sound Components," Proc. of the ASME Design for Manufacturing Conf., Aug. 1996, Irvine, CA.
7. U.S. Patent # 5,121,329, June , 1992.
8. J.W. Comb and W.R. Priedeman, "Control Parameters and Material Selection Criteria for Rapid Prototyping Systems," ibid., Reference #1, Vol. 1993, pp. 86-91.

TABLE I
Binder Components in the RU Series of Binders

Binder Component	Weight % Range	Component Role	Thermal Degradation Temperature Range
Polymer	10 -45	Acts as a backbone	100 - 510 °C
Elastomer	30 - 65	Imparts flexibility	275 - 500 °C
Wax	15 - 50	Viscosity modulator	200 - 500 °C
Tackifier	10 - 40	Promotes adhesion	190 - 475 °C

TABLE II
Physical and Mechanical Properties of GS-44 Parts Processed via Isopressing, Extrusion and FDC

Properties	Isopressed	Extruded	FDC
Green Density*	57%	> 98%	> 96%
Sintered Density (% Theoretical)	> 99%	> 99%	> 98%
Linear Shrinkage	16% in all directions	18% in all directions	X-Y: 16.6 ± 1.3% Z: 19.3 ± 1.6%
4-Point Bend Strength (MPa)	867 ± 50	820 ± 150	824 ± 110
Vickers Indented 3-Point Bend Strength (MPa)	365 ± 5	345 ± 10	354 ± 10

* Iso-pressed green density refers to bulk density of iso-pressed GS-44 without binder. Green densities of extruded and FDC samples correspond to bulk density of samples from 45 volume % RU binder and 55 volume % GS-44 mix. Therefore, GS-44 bulk densities in extruded and FDC samples are >54% and >53%, respectively.
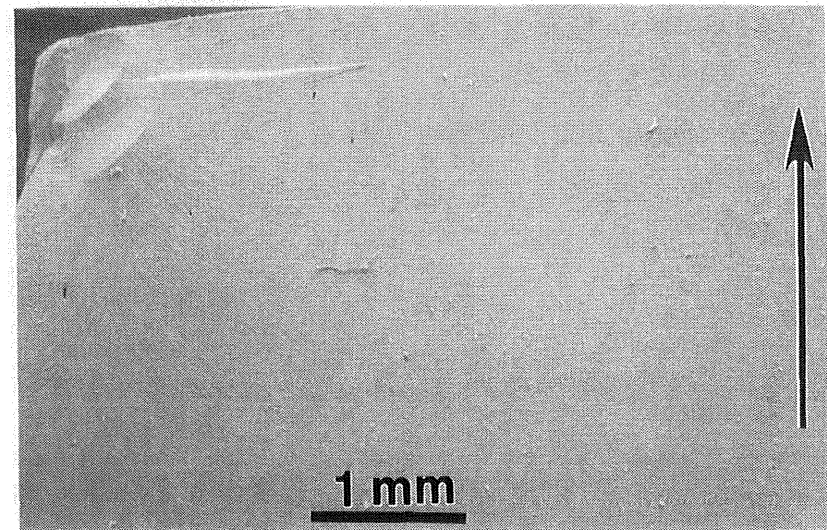

Figure 1: SEM micrograph of a cross section of a green FDC GS-44 part showing no delamination or debonding between adjacent roads and layers (arrow indicates the build direction).
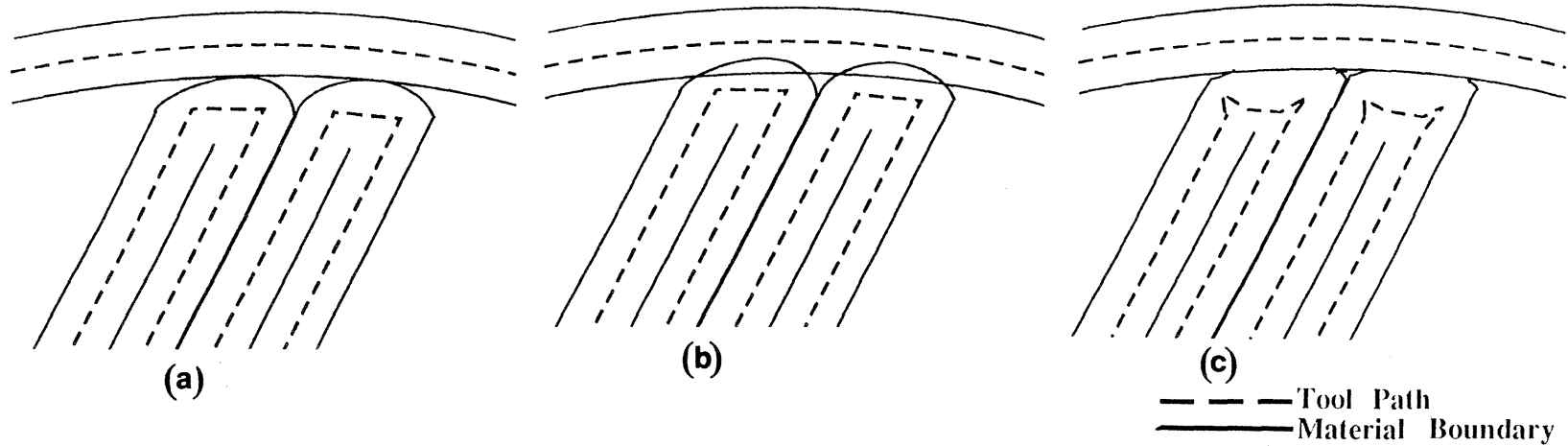
— — — Tool Path
——————Material Boundary

Figure 2: Schematics of raster fill patterns (a) as used in the FDM™ systems showing sub-perimeter voids at the perimeter and raster fill line intersection, (b) with a negative offset for the perimeter showing "plowing" of the raster segment into the perimeter and minimization of the sub-perimeter void, and (c) with altered tool path at the turns near the perimeter showing minimization of the sub-perimeter void.
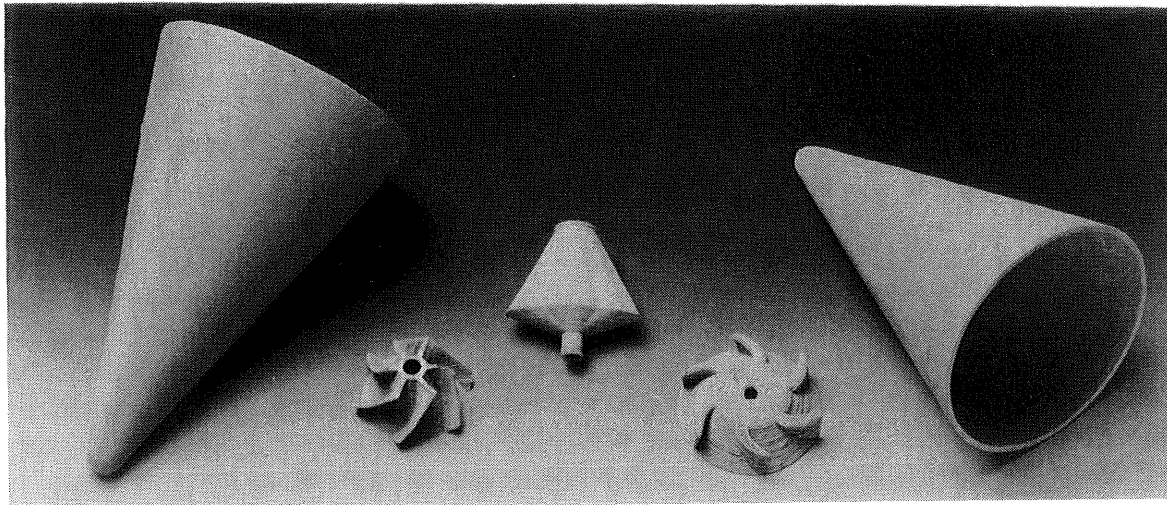

Figure 3: Simple and complex green GS-44 parts, including two tactical missile radome sections, fabricated by FDC processing without the need for build support structures.
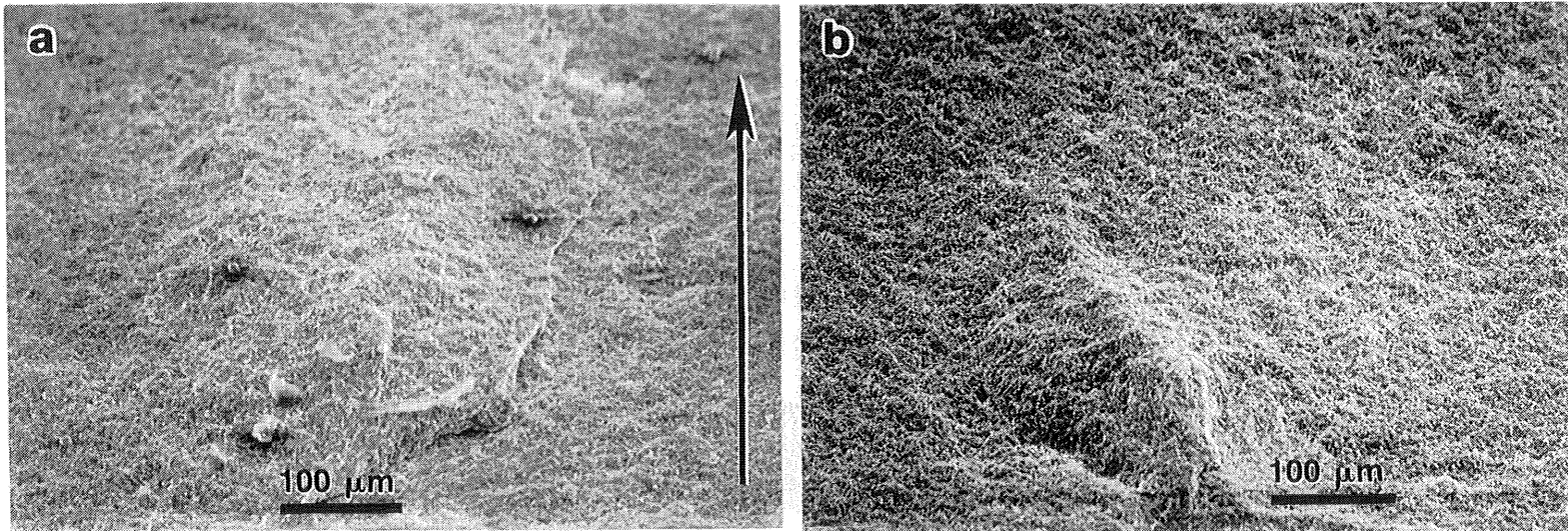
Figure 4: SEM fractographs of indented 3-point bend samples fabricated by (a) FDC (arrow indicates the build direction) and (b) iso-pressing.
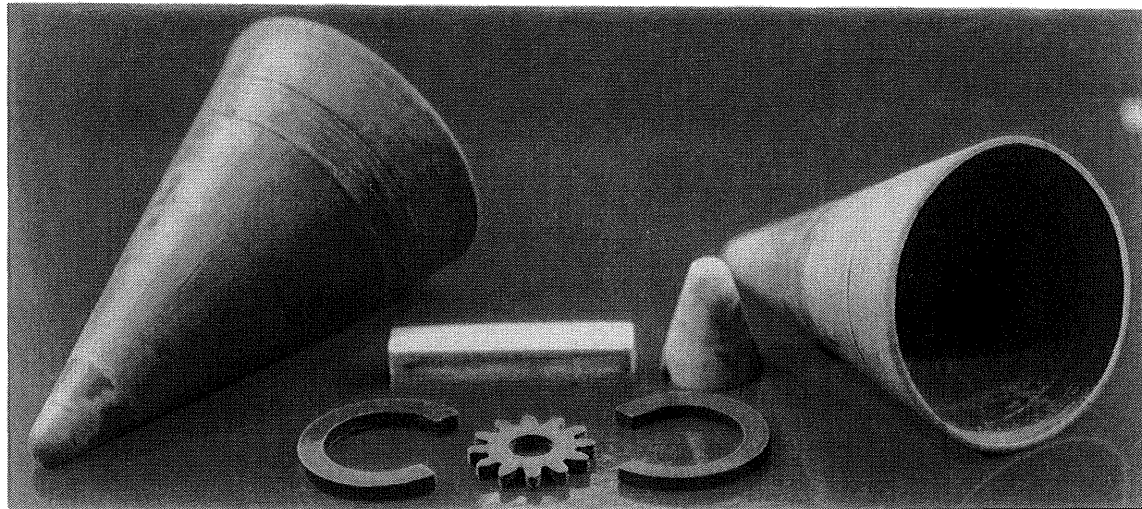

Figure 5: Sintered FDC GS-44 samples, including two tactical missile radome sections.